Pressure Driven Nonmagnetic to Ferromagnetic Transition in CoN

Deepa Kasinathan, W.E. Pickett
Department of Physics, University of California, Davis CA 95616

Calculations of the equation of state for CoN in both rocksalt and zincblende structures indicate the latter is favored at ambient pressure. In the zincblende structure there is no magnetism, whereas the rocksalt phase is ferromagnetic. We predict a first order transition from the zincblende structure to rocksalt at 43 GPa, at which point the moment is about 0.1 μ_B/Co. This pressure-driven nonmagnetic to ferromagnetic transition is not only highly uncommon in itself, but the change is into a magnetic phase that, as a weak ferromagnet, is not far from a ferromagnetic quantum critical point (qcp). The calculated pressure P_{qcp}=176 GPa will be renormalized downward by fluctuations not taken into account.

I. INTRODUCTION

Transition metal oxides comprise perhaps the most thoroughly studied class of solids. Transition metal nitrides, which might be expected to retain several chemical and physical similarities to the oxides, have been studied far less. Although the mononitrides do show substantial structural similarities to the monoxides (rocksalt structure being common in both), their physical properties differ considerably. The main sources of these differences are the electronegativity, which is less for nitrogen than for oxygen, and the fact that nitrogen requires three extra electrons to form a closed shell whereas oxygen requires only two. Thus while insulating behavior, magnetic and metal-insulator transitions under doping, temperature, and pressure, and strongly correlated behavior are the norm in the monoxides, the mononitrides typically are standard metals.

Transition metal pnictides are attracting increased attention recently partially due to the discovery that CrAs can be synthesized in thin film form in the zincblende (B3) structure, and that it is half metallic[1] and therefore a desirable candidate for spintronics applications. Several studies have appeared of transition metal pnictides including nitrides.[2] Although CoN has been known for almost 50 years, originally being reported in the NaCl (B1) phase (but off stoichiometry)[3] and confirmed to be cubic soon after[4], it has attracted little study until recently. The B1 structure was expected since *T*N, *T*= Sc, Ti, V, Cr, share that structure. Much more recently, however, Suzuki, Kaneko *et al.*[5] determined their materials to have the B3 structure, and later Suzuki, Shinohara *et al.*[6] demonstrated that they were Pauli paramagnetic metals. There has been conflicting information for other transition metal nitrides. FeN was reported by Suzuki, Morita *et al.*[7] to have a B3 structure, with evidence of a mictomagnetic state after field cooling. It was later reported by Suzuki, Yamaguchi *et al.*[8] that B3 FeN had no magnetic order down to 2.2 K. The B1 structure, with magnetic order, has also been reported for FeN, as discussed below.

Some time ago thin films of CoN_x were reported by Matsuoka, Ono, and Inukai.[9] Unlike the bulk materials of Suzuki *et al.*, their films were ferromagnetic and they reported hysteresis curves and coercive fields. Being film samples, it was not possible to determine the N concentration precisely or to obtain specific structural details. Very interestingly, the magnetic moment showed a strong perpendicular anisotropy, a property that has long been of great interest to the magnetic recording industry. The source of the magnetism, whether intrinsic, induced by strain, or induced by N vacancies, was not determined.

Theoretical studies of the electronic and magnetic properties of bulk CoN are few and rather cursory. Shimizu *et al.* presented a study[10] of the electronic, structural, and magnetic structure of several of the 3*d* transition metal oxides, but the electronic structure of CoN was only addressed briefly with a rigid band extrapolation from FeN. Eck *et al.* have presented[11] a related theoretical study of 3*d* metal nitrides, again focusing on iron nitrides. Our study of these questions about CoN will extend earlier work on CrN and FeN. CrN transforms to a non-obvious antiferromagnetic phase at 280 K, accompanied by a shear distortion to an orthorhombic structure.[15] This phase is favored only slightly[16] over simple ferromagnetism, with the distortion playing a crucial role. Stoichiometric B1 FeN, on the other hand, was calculated to have a stable ferromagnetic phase,[17] in agreement some experimental data.[18] The difference between CrN and FeN was traced to the smaller ionicity and smaller moment of FeN. Experimentally, both structural choice and the magnetic order may be sensitive to deviations from stoichiometry.

The combination of the structural ambiguity of CoN, of the report of ferromagnetism, and the connection to B3 structure transition metal pnictides that suggest spintronics applications, has led us to make a detailed first principles study of the energetics and magnetism of CoN. We find that B3 CoN is strongly favored over the rocksalt at zero pressure, and we report the bulk modulus B and its pressure derivative for both phases. At 43 GPa pressure we predict a pressure driven nonmagetic-

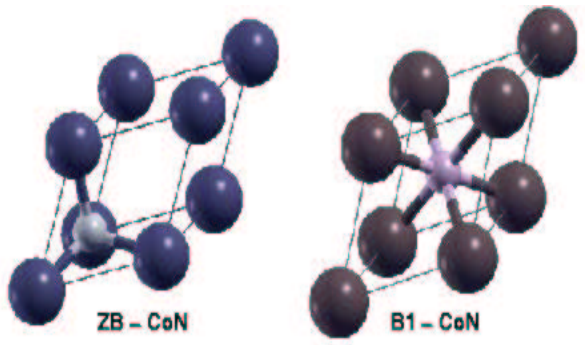

FIG. 1: Structure, illustrating the coordination, of zincblende B3 CoN with tetrahedral coordination (left) and rocksalt B1 CoN with octahedral coordination (right). The big spheres are the Co atoms and the small spheres are the N atoms (although this viewpoint is interchangeable between the atoms). In each case the rhombus shaped primitive cell is pictured.

to-ferromagnetic first order transition to the rocksalt structure, which is unusual in the aspect of being a nonmagnetic-to-magnetic pressure-driven transition. The volume dependence of the moment in the rocksalt structure is illuminated by using fixed spin moment calculations.

II. STRUCTURE AND METHODS

The lattice structures of the B1 and the B3 type CoN are contrasted in Fig. 1. The cobalt atoms in both these structures form an fcc lattice, but differ in the coordinations with the nitrogen atoms. The nearest neighbor N atoms in the B1 structure form an octahedron (sixfold coordinated) about the cobalt atom, while in the B3 structure, N atoms occupy the tetrahedral site (fourfold coordinated). Both the structures are a bipartite "AB" type fcc lattice, with different sublattice positions. The two structures are related by a shift of the N (or Co) sublattice along a (111) direction. The distinct packing types lead to different equal-pressure volumes of around 20%.

All calculations reported here have been performed using the full-potential linearized augmented plane wave code Wien2K[12], using both local density functional (LDA) and generalized gradient approximation (GGA), incorporated in the code for the exchange correlation potential. The muffin tin radii for Co and N have been set to 1.8 and 1.4 a.u. respectively for the ground state and all the high pressure calculations for both B1 and B3 structures. The basis set corresponding to RKmax = 7.0 was used for all calculations. The total energy and density

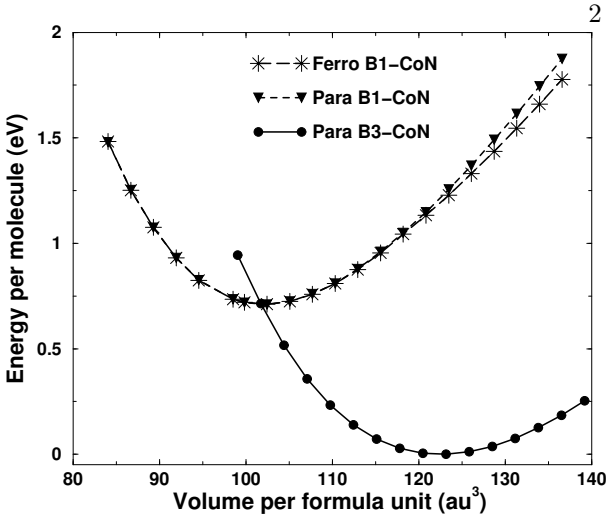

FIG. 2: Calculated equations of state of CoN for the non-magnetic zincblende structure and both nonmagnetic and ferromagnetic B1 structure. The zincblende phase is the stable one at ambient pressure by almost 0.75 eV per cell.

of states (DOS) calculations were done with more than 1000 k-points in the irreducible ($\frac{1}{48}$) wedge of the Brillouin zone to attain good energy and charge convergence. The DOS has been calculated using the tetrahedral integration method. The energies were iterated to within 10^{-6} Rydberg convergence and the magnetic moments to within $0.01\mu_B$.

III. EQUATION OF STATE

A. Equation of State in LDA

To obtain the structural and magnetic properties of CoN, we performed total energy calculations using the LDA functional of Perdew and Wang[13] by varying the volumes for the non-magnetic B3 structure and both nonmagnetic and ferromagnetic B1 structure. The volumes were varied from $0.74V_\circ$ to $1.04V_\circ$ for the B3 case and from $0.64V_\circ$ to $1.04V_\circ$ for the B1 case. $V_\circ$ is the experimental equilibrium volume[5] of $a_\circ^3/4 = 134.3$ a.u.^{3} ($a_\circ$=4.297 Å). Results using the GGA functional will be presented in a following subsection.

The equations of state E(V) for the three cases are plotted in Fig. 2. Contrary to the claim by Shimizu *et al.*[10] but in agreement with the conclusion of Eck *et al.*[11], the total energy of B3 CoN is lower than that of B1 CoN, thereby making the tetrahedrally coordinated structure stable at ambient temperature and pressure. The calculated equilibrium B1 lattice

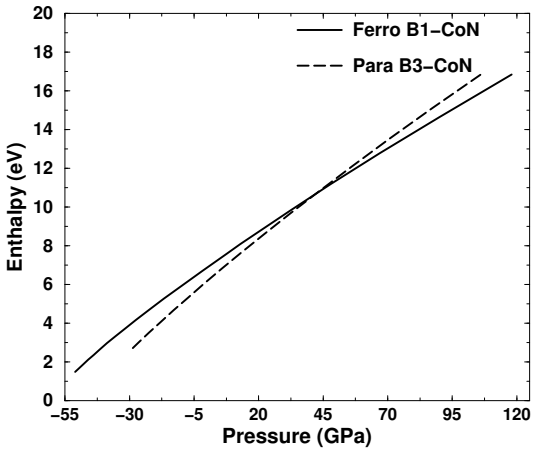

FIG. 3: Plot of the enthalpy E+PV versus pressure for both phases of CoN, illustrating its continuity at the critical pressure P_c for the first order structural transition. Finding where the enthalpies are equal avoids having to perform the common-tangent construction to obtain P_c.

constant is 4.17 $\mathring{A}$, 3% smaller than the experimental value[5] $a_\circ$= 4.297 $\mathring{A}$. For the B1 structure, the energy of the ferromagnetic state is lower than the nonmagnetic state for all volumes. Therefore, if B1-CoN is prepared, it will favor a magnetically ordered ground state. The equilibrium B1 lattice constant and magnetic moment are 3.92 $\mathring{A}$ and 0.22 μ_B respectively. The equilibrium volume for the B1 structure is 17% smaller than the B3 structure, reflecting the openness of the B3 structure. The possibility of magnetic order in the B3 structure was also investigated. Fixed spin moment calculations on this system showed no tendency to magnetism.

B. Transition Pressure

The equation of state E(V) curves shown in Fig. 2 indicate a phase transition from the non-magnetic B3 phase to the ferromagnetic B1 phase under pressure. To facilitate the calculation of the transition pressure, the total energies were fitted to an equation of state. We have used Taylor series, Birch,[19] and Murnaghan[20] equations of state to compare the consistency of the values obtained. Here, we report the results of just the Birch fitting

$$E(V) = E_c + \frac{9}{16}BV_\circ\left[v^{-2}\left(B^{'}-4\right) + \left(3B^{'}-16\right)v^{-\frac{2}{3}} + \left(14-3B^{'}\right)v^{-\frac{4}{3}}\right]$$

$V_\circ$ represents the equilibrium volume of the unit cell, B is the bulk modulus and $B^{'}$ is its pressure derivative, both calculated at $V_\circ$. E_c is a constant and $v \equiv V/V_\circ$. The pressure is obtained by taking the volume derivative of the above equation. The next step is to calculate the enthalpy $E + PV$ of the two systems and the transition pressure (P_c) is the one at which the enthalpies are equal. The enthalpy-pressure relationship is presented in Fig. 3 for both paramagnetic B3-CoN and ferromagnetic B1-CoN. The curves cross at P_c = 41 GPa. There is a 15% volume collapse at this pressure, where the structure changes from B3 to the denser (and magnetic) B1 phase.

TABLE I: Bulk modulus B (GPa) and its pressure derivative $B^{'}$, contrasting LDA and GGA results. GGA gives a larger volume and a corresponding softer lattice as usual.

	LDA		GGA	
	B	B'	B	B'
B1 CoN	347	5.4	275	4.8
B3 CoN	305	4.5	260	4.2

C. Corresponding Results using GGA

It is generally found that the GGA functional for the exchange-correlation energy gives a more accurate equilibrium volume and equation of state than does LDA. For this reason all the total energy calculations were repeated using the GGA functional of Perdew, Burke, and Ernzerhof.[14] The calculated equilibrium lattice constants are (quoting GGA versus LDA): 4.25 Å versus 4.17 Å for the B3 phase, a 1.9% increase; 4.02 Å versus 3.92 Å for the rocksalt phase, a 2.5% increase. Thus GGA brings the calculated lattice constant to within 1% of the experimental value.

Applying the same procedures as described above to get enthalpy-pressure relationships, the transition pressure was increased from 41 GPa (LDA) to 43 GPa (GGA). This small change reflects that the volume increase given by GGA is similar for the two crystal structures, leaving a common tangent (whose slope is -P_c) with little change. The equilibrium moment of the ferromagnetic B1-CoN is 0.12 μ_B in GGA, roughly half of the LDA value in spite of the larger volume. This decrease was unexpected, since simple increase of the volume usually decreases the bandwidth and increases the tendency toward magnetism as reflected in the enhanced magnetic moment.

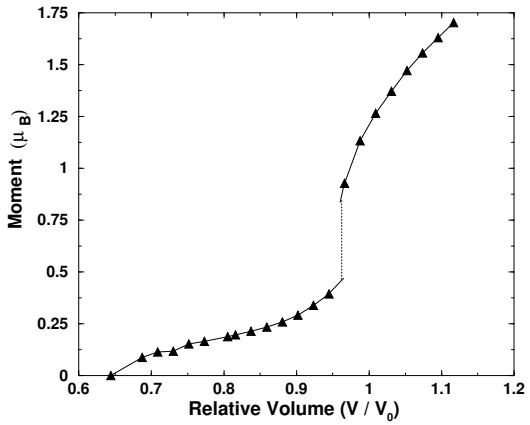

FIG. 4: Moment versus volume relationship for ferromagnetically ordered B1 CoN. Around the critical volume of 0.98V$_o$ the moment collapses from 0.9 to 0.4 μ_B. The corresponding energy curve E(M) from the fixed spin moment method is shown in Fig. 5. The equilibrium volume V$_\circ$ is given in the text.

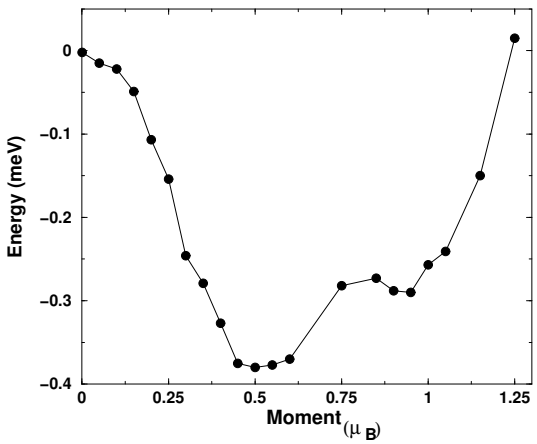

FIG. 5: The energy versus fixed (imposed) spin moment for rocksalt CoN at 0.97V$_o$. The double minimum structure reveals the cause of the moment collapse in Fig. 4: as the volume changes, the positions of the minima remain fixed but the energies at the minima change, and the volume at which the minima are degenerate marks the critical volume. Note the very small energy scale, which accounts for the calculated values not lying on a completely smooth curve.

IV. MOMENT COLLAPSE IN THE ROCKSALT PHASE

Applying pressure to any structure with magnetic order increases the bandwidth and almost always decreases the moment of the system. Figure 4 shows the moment vs. volume M(V) curve of the ferromagnetic B1 CoN phase. A striking feature of M(V) is the collapse of the moment around 0.98 V$_o$, which results from a first order magnetic transition where the moment jumps from 0.9 μ_B to 0.4 μ_B. To better understand the mechanism of collapse of the moment, we carried out fixed spin moment calculations[21] for the 0.97 V$_o$ case. The resultant energy vs. moment is plotted in Fig. 4. We observe two energy minima for the system with very small energy difference. As the volume changes, the energies if these two local minima vary, and where they become equal a first order magnetic transition occurs. In this case it is a moment collapse, 0.9 $\rightarrow$ 0.4 μ_B. Note that this volume range is where the B3 structure is stable, hence this collapse is not accessible to experiment.

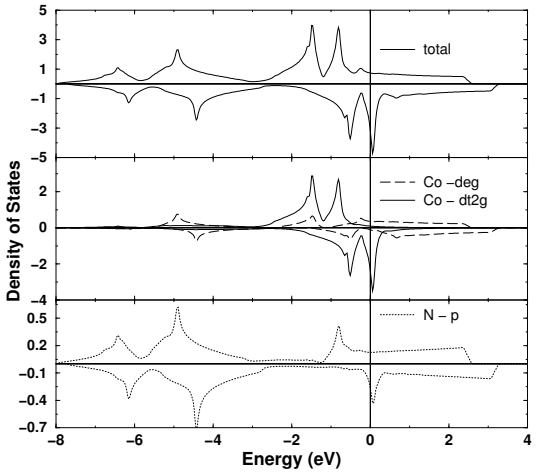

FIG. 6: Total and partial density of states (DOS) of ferromagnetic rocksalt structure CoN for V = 0.96 V$_\circ$. *Top panel*: total DOS; the peak in the minority (plotted downward) states is responsible for the moment collapse (see text). Middle panel: Co e_g and t_{2g} DOS, illustrating that the peak is due to the t_{2g} states. *Bottom panel*: the N 2p DOS, illustrating strong hybridization with both e_g and t_{2g} states of Co.

From the plot of the density of states in the high moment phase at 0.96V$_\circ$ in Fig. 6, one can see a peak very close to and above the Fermi energy for the minority spin. The contribution to that peak arises from Co t$_{2g}$ states. Applying pressure to reduce the volume (which decreases the magnetization) moves the peak to lower energy, thereby bringing the peak of the Co t$_{2g}$ states right on top of the Fermi energy. This high density of states at the Fermi energy is energetically unfavorable enough that the system undergoes a first order transition to move the peak below the Fermi energy, rather than to move the Fermi level precisely onto the peak. This jump in the filling of states changes the moment discontinuously, thus

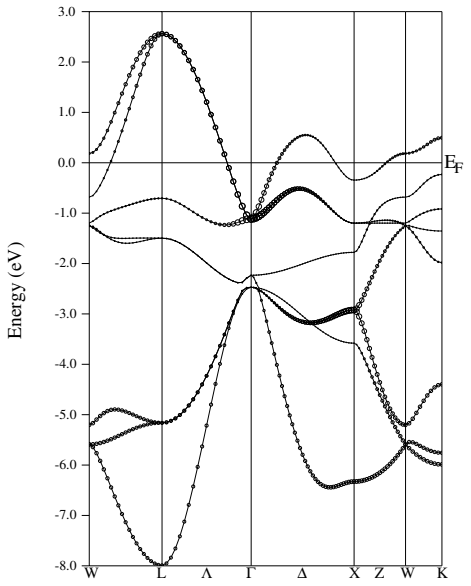

FIG. 7: Majority band structure of ferromagnetic B1 CoN along high symmetry directions. The symbol size if proportional to the N $2p$ character. As discussed in the text, N $2p$ character is excluded from the region -2.5 eV to -1.3 eV by $t_{2g} - 2p$ mixing and resulting repulsion.

revealing the driving force for the moment collapse. The energy barrier is quite small, ∼0.1-0.2 meV/cell, accounting for our failure to observe hysteresis.

It is worthwhile to clarify an unexpected feature in the DOS of Fig. 6, the lack of N $2p$ character in the energy region -3 eV to -1 eV in the majority bands, and the corresponding region about 1 eV higher in the minority DOS – this is the lower of the two t_{2g} DOS peaks. This void is unexpected because the N $2p$ states clearly do mix with the Co t_{2g} states as is clear from the corresponding peaks in the respective DOS in Fig. 6 (near -1 eV in the majority, and the important peak at E_F in the minority that was discussed above). To illustrate the origin of the effect, the majority bands are presented in Fig. 7 with N $2p$ character emphasized. At the zone center Γ, the $3d$ and $2p$ states are close in energy with the $3d$ states lying below the $2p$ states. The $2p - e_g$ hybridization is large, and it results in the 10.5 eV total bandwidth. The t_{2g} bandwidth itself is narrow, less than 2 eV as shown in Fig. 6, and the coupling tends primarily to repel the N $2p$ character away, and $2p - t_{2g}$ hybridization survives only in the upper of the two t_{2g} peaks.

V. CONCLUSIONS

This study has cleared up several features in the experimental data for CoN. From total energy calculations, it has been established that CoN takes a paramagnetic zincblende structure at ambient pressure, rather than rocksalt as sometimes suggested. Around 43 GPa we predict a first order phase transition to the denser rocksalt phase, which at this volume has a small but clearly nonvanishing ferromagnetic moment of 0.1 μ_B per Co. Thus pressure drives the system into a weak ferromagnetic phase that is relatively close to a quantum critical point (QCP). Our calculations predict this QCP, where the Curie temperature finally goes to zero, to be $P_{qcp} = 176$ GPa. Fluctuations should renormalize P_{qcp} to a lower value.

Our work has not explained the observation of ferromagnetic films by Matsuoka *et al.*[9] Strain, nonstoichiometry, or even the altered chemistry of the open-shell transition metal atom and the N atom at the surface, may be factors. Strain can change the in-plane lattice constant, however the tendency to conserve volume will cause the perpendicular lattice constant to compensate and there may be much less reduction in volume than the in-plane lattice alone would suggest. Nonstoichiometry is an obvious concern; since Co itself is ferromagnetic, regions with decreased N content, or N-free Co clusters, will tend to be ferromagnetic. Finally, even at perfect stoichiometry, the presence of the surface can alter the chemistry considerably. At the Mn-terminated (001) surface of $CaMnO_3$, for example, the coupling between subsurface and surface Mn ions was found to become ferromagnetic,[22] rather than the antiferromagnetic coupling of the bulk. It is likely to require further study both experimentally and theoretically to resolve the origin of the magnetism of CoN films.

VI. ACKNOWLEDGMENTS

We acknowledge helpful conversations with J. Kuneš, B. Maddox, A. K. McMahan, R. T. Scalettar, and C.-S. Yoo. D. K. was supported by Department of Energy Grant DE-FG03-01ER45876. W. E. P. acknowledges support from the Department of Energy's Stewardship Science Academic Alliances Program through Grant DE-FG03-03NA00071.

[1] H. Akinaga, T. Manago, and M. Shirai, Jpn. J. Appl. Phys. Part 2, **39**, L1118 (2000).

[2] See J. E. Pask, L. H. Yang, C. Y. Fong, W. E. Pickett, and S. Dag, Phys. Rev. B **67**, 224420 (2003) and references therein.

[3] O. Schmidtz-Dumont and N. Kron, Angew. Chem. **67**, 231 (1995).

[4] B. Taylor, B. Joyner, and F. H. Verhoek, J. Am. Chem. Soc. **83**, 1069 (1961).

[5] K. Suzuki, T. Kaneko, H. Yoshida, H. Morita, and F. Fujimori, J. Alloys Compds. **224**, 232 (1995).

[6] K. Suzuki, T. Shinohara, F. Wagatsuma, T. Kaneko, H. Yoshida, Y. Obi, and S. Tomiyoshi, J. Phys. Soc. Japan **72**, 1175 (2003).

[7] K. Suzuki, H. Morita, T. Kaneko, H. Yoshida, and H. Fujimori, J. Alloys Compds. **201**, 11 (1993).

[8] K. Suzuki, Y. Yamaguchi, T. Kaneko, H. Yoshida, Y. Obi, H. Fujimori, and H. Morita, J. Phys. Soc. Japan **70**, 1084 (2001).

[9] M. Matsuoka, K. Ono, and T. Inukai, IEEE Trans. on Magnetics, Vol. MAG-23, 2788 (1987).

[10] H. Shimizu, M. Shirai, and N. Suzuki, J. Phys. Soc. Japan **66**, 3147 (1997).

[11] B. Eck, R. Dronskowski, M. Takahashi, and S. Kikkawa, J. Mater. Chem. **9**, 1527 (1999).

[12] P. Blaha, K. Schwarz, G. K. H. Madsen, D. Kvasnicka, and J. Luitz, J. Phys. Chem. Solids **63**, 2201 (2002).

[13] J. P. Perdew and Y. Wang, Phys. Rev. B **45**, 13244 (1992).

[14] J. P. Perdew, S. Burke, and M. Ernzerhof, Phys. Rev. Lett. **77**, 3865 (1996).

[15] P. Subramanya Herle, M. S. Hedge, N. Y. Vasathacharya, and S. Philip, J. Solid State Chem. **134**, 120 (1997) and references therein.

[16] A. Filippetti, W. E. Pickett, and B. M. Klein, Phys. Rev. B **59**, 7043 (1999).

[17] A. Filippetti and W. E. Pickett, Phys. Rev. B **59**, 8397 (1999).

[18] See Ref.17 for references to the literature on FeN.

[19] F. Birch, J. Geophys. Res. **83**, 1257 (1978).

[20] F. D. Murnaghan, Proc. Natl. Acad. Sci. U.S.A. **30**, 244 (1944).

[21] K. Schwarz and P. Mohn, J. Phys. F **14**, L129 (1984); G. L. Krasko, Phys. Rev. B **36**, 8565 (1987).

[22] A. Filippetti and W. E. Pickett, Phys. Rev. Lett. **83**, 4184 (1999).